The Astronomical Journal, 121:1583–1596, 2001 March

CCD SPECKLE OBSERVATIONS OF BINARY STARS FROM THE SOUTHERN HEMISPHERE. III. DIFFERENTIAL PHOTOMETRY

Elliott Horch[1,2] and Zoran Ninkov
Chester F. Carlson Center for Imaging Science, Rochester Institute of Technology, 54 Lomb Memorial Drive, Rochester, NY 14623-5604; horch@cis.rit.edu, ninkov@cis.rit.edu

and

Otto G. Franz[1]
Lowell Observatory, 1400 W. Mars Hill Road, Flagstaff, AZ 86001; ogf@lowell.edu
Received 2000 November 20; accepted 2000 January 9

ABSTRACT

Two hundred seventy-two magnitude difference measures of 135 double star systems are presented. The results are derived from speckle observations using the Bessel V and R passbands and a fast readout CCD camera. Observations were taken at two 60 cm telescopes, namely the Helen Sawyer Hogg Telescope, formerly at Las Campanas, Chile, and the Lowell-Tololo Telescope at the Cerro Tololo Inter-American Observatory, Chile. The data analysis method is presented and, in comparing the results to those of *Hipparcos* as well as to recent results using adaptive optics, we find very good agreement. Overall, the measurement precision appears to be dependent on seeing and other factors but is generally in the range of 0.10–0.15 mag for single observations under favorable observing conditions. In four cases, multiple observations in both V and R allowed for the derivation of component $V-R$ colors with uncertainties of 0.11 mag or less. Spectral types are assigned and preliminary effective temperatures are estimated in these cases.

Key words: binaries: close — binaries: visual — techniques: interferometric — techniques: photometric

1. INTRODUCTION

Binary stars remain a fundamental tool in understanding stellar structure and evolution, largely because stellar mass estimates can be derived from orbital information. In the first two papers of this series, relative astrometry was presented for double star systems observed by way of speckle interferometry at the Helen Sawyer Hogg Telescope, which at the time was located at the University of Toronto Southern Observatory, Las Campanas, Chile (Horch, Ninkov, & Slawson 1997, hereafter Paper I), and the Lowell-Tololo Telescope at the Cerro Tololo Inter-American Observatory (CTIO) (Horch, Franz, & Ninkov 2000, hereafter Paper II). Such observations are a necessary step in determining the masses of the components, which in turn can be compared with theoretical models. However, empirically determined masses become much more useful when they are combined with other information about the components, such as luminosity and/or effective temperature. This highlights the importance of observationally determined magnitude and color information of the individual stars in binary systems.

Determining reliable magnitude differences with speckle interferometry has proved difficult. One of the most successful attempts to date was the fork algorithm of Bagnuolo (1988), which was subsequently used to determine the component magnitudes of the Capella system (Bagnuolo & Sowell 1988) and of bright Hyades cluster binaries (Dombrowski et al. 1990). However, the degree of success in these cases is due to the brightness of the systems, and the technique has not been successfully applied to speckle interferometry data in general. The current state of affairs was summarized in Hartkopf et al. (1996), where the authors stated that uncertainties of 0.5 mag are generally assigned for magnitude difference estimates. This situation is sometimes referred to as the "magnitude difference problem" of speckle interferometry. More recently, attempts to produce good component magnitudes have been made using adaptive optics (ten Brummelaar et al. 1996, 1998, 2000; Roberts 1998; Barnaby et al. 2000). This process has also turned out to be surprisingly nontrivial, and, for example, the method now used by ten Brummelaar et al. involves taking numerous short exposure images of a binary system with the adaptive optics system turned on and then using a shift-and-add technique to derive a final resolved image. Typical uncertainties in the magnitude differences of ± 0.05 to ± 0.10 per observation can be obtained in this way, and these data do not appear to exhibit systematic offsets when compared with other results such as those from *Hipparcos*, a distinct improvement over the situation in the past with regard to speckle data.

The challenge of obtaining magnitude differences from speckle interferometry consists of two main difficult calibration problems. First, detectors used for most visible-light speckle observations are microchannel–plate-based devices that are inherently nonlinear. The physical characteristics of the microchannel plate such as the pulse height distribution and the channel recharge time constant are usually not known, preventing effective calibration attempts. Second, the atmosphere and the small field of view used can produce systematic errors in the magnitude difference that are known to be a function of the separation of the two stars but are in general poorly understood. In this paper, we present a simple, robust data reduction method developed for bare (unintensified) CCD speckle data that can be used to obtain reliable magnitude difference estimates. The use of a linear detector effectively eliminates the first problem, and

[1] Visiting Astronomer, Cerro Tololo Inter-American Observatory, National Optical Astronomy Observatories.

[2] Visiting Astronomer, University of Toronto Southern Observatory, Las Campanas, Chile.

the data reduction method is designed to reduce the second, insofar as it is possible. We then apply the technique to the two data sets presented in Papers I and II and analyze the measurement precision.

2. OBSERVATIONS AND DATA REDUCTION

Detailed descriptions of the observations and the data taking methods can be found in Papers I and II. In both cases, speckle interferograms were recorded with a Kodak KAF-4200 CCD set in a Photometrics camera head and operating in fast subarray readout mode. The subarray size gave a field of view of approximately $6''.4 \times 12''.8$, which is somewhat larger than is normally used in speckle work. A typical observing sequence consisted of recording 1024 frames on the object of interest (with an exposure time of typically 30 ms per frame), followed by a similar observation of a bright unresolved star near the object of interest on the sky, chosen from The Bright Star Catalogue (Hoffleit & Jaschek 1982). These observations allow us to deconvolve the speckle transfer function from the observed binary power spectrum, thus obtaining the "true" object power spectrum. The data presented here come from the 1997 February run at Las Campanas (astrometry for the same data is presented in Paper I), and the 1999 October run at CTIO (astrometry presented in Paper II). Seeing conditions during the former run averaged $1''.2$, whereas in the latter case, the seeing was significantly worse, averaging $1''.9$. On the Las Campanas run, the Bessel V passband was used exclusively, and at CTIO, both the Bessel V and R filters were used (Bessel 1990).

The astrometric reduction method is a weighted least squares fit to the true binary power spectrum. Trial fit functions are of the general form

$$f(\boldsymbol{u}) = A^2 + B^2 + 2AB \cos\,[2\pi(\boldsymbol{x}_A - \boldsymbol{x}_B)\cdot\boldsymbol{u}]\,, \qquad (1)$$

where A and B represent the irradiances of the primary and secondary, respectively, and $\boldsymbol{x}_A - \boldsymbol{x}_B$ represents the vector separation of the binary on the image plane. For astrometric data reductions, the final vector separation obtained from the best fit match to the data is then converted into a separation and position angle and the irradiance values are discarded. However, an irradiance ratio, B/A, and its formal error are stored in a summary results file created along with the final astrometry. For the photometric analysis here, we have simply taken these irradiance ratios to arrive at magnitude difference estimates, via the standard formula

$$\Delta m = m_B - m_A = 2.5 \log \frac{A}{B}\,. \qquad (2)$$

A formal error in the magnitude difference can likewise be derived. Typically, these formal errors significantly underestimate the measurement uncertainty due to the presence of systematic errors, and we discard these values. For example, the deconvolution process is a source of measurement error. In order to determine the level of uncertainty generated, we have performed tests where the same binary power spectrum is deconvolved by a series of different point sources. We find that the typical rms scatter introduced in the magnitude difference is about 0.05 mag, which alone is usually much larger than the formal errors of a particular fit, though still smaller than the total measurement uncertainty. The overall precision of our measures is discussed fully in § 3.2.

The magnitude difference estimates are also susceptible to some of the systematic errors alluded to in the introduction. In particular, it is expected that as the separation of the two stars in a binary system increases, the speckle pattern generated by the secondary will begin to fall outside the isoplanatic patch of the primary star. As a consequence, the pattern will cease to be identical to that of the primary, and a loss of correlations will result in the autocorrelation function at the locations corresponding to the positive and negative vector separations of the two components. This in turn will lead to an overestimate of the magnitude difference. As discussed in Dainty (1984), the size of the isoplanatic angle, $\delta\omega$ is given by

$$\delta\omega \approx 0.36\,\frac{r_0}{\Delta h}\,, \qquad (3)$$

where r_0 is the Fried parameter and Δh is a measure of the dispersion of the turbulent layers. On the other hand, the seeing, ω, is also related to the Fried parameter, by the following:

$$\omega = \frac{\lambda}{r_0}\,, \qquad (4)$$

where λ is the wavelength of the observation. Therefore, we may approximate the isoplanatic angle in terms of the seeing as

$$\delta\omega \approx 0.36\,\frac{\lambda}{\omega\Delta h}\,. \qquad (5)$$

A measure of "isoplanicity" of the observation can then be obtained by forming the dimensionless parameter q

$$q = \frac{\rho}{\delta\omega} \approx \frac{\rho\omega\Delta h}{0.36\lambda} \propto \rho\omega\,, \qquad (6)$$

where $\rho = |\boldsymbol{x}_A - \boldsymbol{x}_B|$ is the separation of the two stars. For small values of q, the degree of isoplanicity should be high, indicating nearly perfect correlation between primary and secondary speckle patterns, whereas for high values, the secondary speckle pattern will be sufficiently different from that of the primary to produce a significant systematic error in the magnitude difference derived. We suggest that the quantity $q' \equiv \rho\omega$, which can easily be derived from our data, is therefore a useful parameter in determining if reliable photometry can be obtained from a given speckle observation.

Many of the objects discussed in Papers I and II have magnitude difference estimates obtained by *Hipparcos* and listed in the *Hipparcos* Catalogue (ESA 1997). In Figure 1, the differences between our ΔV results and the *Hipparcos* results are plotted against the product of the seeing and the object separation, as determined in the astrometric analysis for all systems in Papers I and II having *Hipparcos* magnitude differences. At low ($q' < 2$) values of this parameter, there appears to be little or no systematic offset compared to the *Hipparcos* values. However, as expected from the preceding discussion, at larger values of q', there is a systematic trend toward larger derived speckle magnitude differences, relative to the *Hipparcos* results. For the results presented in the remainder of this paper, we have only considered observations with $q' < 2$. It may eventually be possible to predict the shape of this curve and correct even large-q' magnitude difference results accordingly, but a

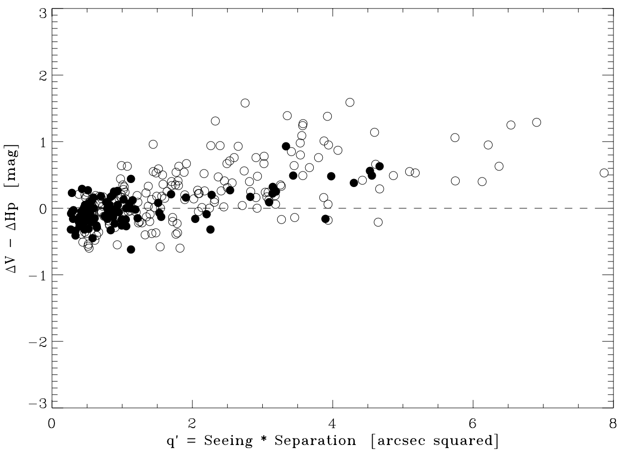

FIG. 1.—Magnitude-difference differences for our measures vs. *Hipparcos* measures, as a function of $q' = \rho\omega$, the product of the seeing and the system separation for the observation. Filled circles indicate data from the Las Campanas run, and open circles are points from the CTIO run.

careful analysis would not only need to include the degree of isoplanicity, but also the effect of limited field of view. Accounting for photons that fall outside the field of view and remain undetected would involve considerations such as the seeing, detector orientation, and object placement and could in general lead to an overestimate or an underestimate of the magnitude difference. The interplay between these effects is currently under investigation, but the approach taken here simply includes an observation if the effect of nonisoplanicity can reasonably be assumed to be minimized and relies on our comparatively large field of view to minimize the effect of undetected photons. The magnitude differences presented in the next section are therefore obtained in the same way as our process for obtaining astrometry but are subject to the further quality control criterion that the product of the seeing times separation is less than 2.

3. RESULTS

3.1. *Measures*

Tables 1, 2, and 3 contain the main body of photometric results from the data sets. In Table 1 we present V-band measures from the Las Campanas data, in Table 2 the V-band measures from CTIO, and in Table 3 the R-band measures from CTIO. In all three cases, the columns give (1) in order of availability, the Aitken Double Star (ADS) Catalogue number, or the Bright Star Catalogue (HR) number, or the Durchmusterung (BD, CP, or CD) number; (2) the discoverer designation; (3) the HD number; (4) the *Hipparcos* Catalogue number; (5) the right ascension and declination in J2000.0 coordinates, which is the same as the identification number in the Washington Double Star (WDS) Catalogue (Worley & Douglass 1997) for all objects that have WDS entries; (6) the observation date in fraction of the Besselian year; and (7) the speckle magnitude difference. Table notes appear for systems whose quadrant determination from the astrometric analyses in Papers I and II was ambiguous and/or inconsistent with previous measures in the Third Catalogue of Interferometric Measures of Binary Stars (Hartkopf, McAlister, & Mason 1997). In such cases, our quadrant determinations may of course be reconciled with those in the Third Catalogue simply by reversing the sign of the magnitude difference; this may be appropriate in the case of small-Δm systems. Two objects in the tables, noted with asterisks, did not have previous astrometric data given in Papers I and II; we give the position angles and separations determined here in the table notes. The measures are shown without uncertainty estimates, but as discussed fully in the next section, we believe the uncertainties of individual observations to be approximately 0.15 mag in general for the Las Campanas observations, and between 0.15 and 0.30 mag in the case of the CTIO data. No corrections have been made for interstellar reddening or the wavelength dependence of the atmospheric transmission; both are assumed to be negligible in this work. In the latter case, an analysis was completed using a standard atmospheric transmission curve which indicated that even in the case of extreme color differences of binary components and large air mass, systematic offsets of less than 0.02 mag are obtained by not properly accounting for the true atmospheric transmission. More typical offsets were less than 0.01 mag.

3.2. *Measurement Precision*

3.2.1. *Comparison with Hipparcos Data*

We first estimate the precision of measures appearing in Tables 1 and 2 by comparing our results with those of *Hipparcos*. In Figure 2, our V-band magnitude differences are plotted against the magnitude differences listed in the *Hipparcos* Catalogue for all *Hipparcos* objects observed. The *Hipparcos* observations were taken in the so-called H_p band and not in the Bessel V filter; H_p is both broader and bluer than V. For main-sequence stars, one therefore expects a slightly larger value for the magnitude difference in the case of the *Hipparcos* results, though the correlation between the two systems should be high. This is consistent with the appearance of Figure 2. For systems in which we derive a magnitude difference of less than 0.2 mag, we have included the quadrant information from Papers I and II by plotting the negative of the ΔV value appearing in our tables here in cases where the quadrant was inconsistent with determinations of other observers. In other words, for these cases we have assumed that the error in quadrant determination is ours and should be reflected also in the

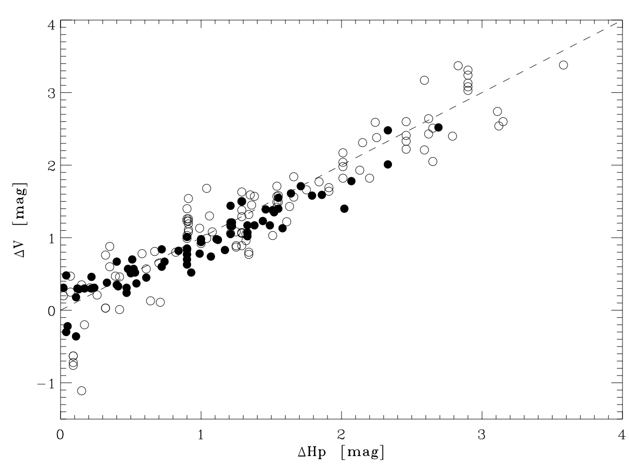

FIG. 2.—V-band speckle magnitude differences plotted against the magnitude difference appearing in the *Hipparcos* Catalogue for systems in Tables 1 and 2. Filled circles are data points from the Las Campanas observations, and open circles are data points from CTIO.

TABLE 1

SPECKLE *V*-BAND DIFFERENTIAL PHOTOMETRY MEASURES, LAS CAMPANAS

HR,ADS DM, etc. (1)	Discoverer Designation (2)	HD (3)	HIP (4)	WDS (α,δ J2000.0) (5)	Date (1900+) (6)	ΔV (7)
ADS 3588	BU 314AB	31925	23166	04590−1623	97.1005	1.55
					97.1170	1.40
ADS 3799	STT 517AB	33883-4	24349	05135+0158	97.1224	0.45
ADS 3974	A 486	35261	25171	05231−0806	97.1225	1.13
CD−33 2419......	HU 1393	37224	26245	05354−3316	97.0951	1.07
					97.1006	1.02
					97.1170	1.17
ADS 4241	BU 1032AB	37468	26549	05387−0236	97.1171	1.18
					97.1225	1.16
					97.1225	1.05
					97.1225	1.44
CD−48 1991......	I 63AB	39177	27408	05482−4855	97.0952	1.50
ADS 4817	B 104	42899	29449	06123−2515	97.0899	0.82
ADS 4971	A 2667	44333	30217	06214+0216	97.1171	1.17
CD−35 3008......	I 1118	47229	31521	06360−3510	97.1198	1.59[a]
HR 2468	I 5AB	48189	31711	06380−6132	97.1199	2.48
CP−61 706	I 6	49076	—	06425−6145	97.0953	0.42
					97.1172	0.25
CD−28 3591......	RST 1329	51202	33270	06552−2902	97.0953	1.40
HR 2612	I 65	51825	33451	06573−3530	97.1172	0.33
ADS 5712	BU 573	52694	33869	07018−1053	97.1226	0.70
ADS 5925	BU 575AB	56012	35035	07148−1529	97.1226	0.30[c]
CD−46 3046......	I 7	57095	35296	07175−4659	97.1227	1.16
ADS 6084	SEE 79	58846	—	07263−2810	97.1227	0.44
HR 2937	FIN 324AB-C	61330	37096	07374−3458	97.1172	1.38
CD−42 3396......	I 353	61946	37318	07397−4317	97.0900	0.60
					97.0954	0.84
ADS 6315	HU 710	62351	37608	07430−1704	97.0900	0.51
					97.1172	0.55
CD−46 3421......	HU 1428	63449	37953	07468−4648	97.1227	0.97
ADS 6420	BU 101	64096	38382	07518−1354	97.0954	1.01
					97.1173	0.83
					97.1173	0.85
					97.1200	0.77
					97.1200	0.77
					97.1227	0.63
					97.1227	0.70
HR 3234	SEE 96Aa-B	68895	40183	08125−4616	97.0955	1.21
HR 3335	B 2179	71581	41475	08276−2051	97.1173	1.58
ADS 6871	BU 205AB	72626	41949	08331−2436	97.1201	0.30
ADS 6914	BU 208AB	73752	42430	08391−2240	97.1174	1.39
ADS 6993	SP 1AB	74874	43109	08468+0625	97.1174	1.07
					97.1174	0.78
					97.1174	0.89
					97.1201	0.95
					97.1201	1.00
					97.1228	1.22
					97.1228	0.99
CD−32 6023......	RST 2599	77920	44527	09044−3306	97.1229	0.52
CD−45 4982......	I 11	79900	45413	09152−4533	97.0901	0.98
					97.1175	0.94
ADS 7382	A 1588AB	81728	46365	09272−0913	97.1202	0.12
CD−39 5580......	COP 1	82434	46651	09307−4028	97.1175	1.21
HR 3840	SEE 115	83520	47204	09372−5340	97.1229	0.36[c]
HR 3844	I 202	83610	47328	09387−3937	97.1202	1.78
ADS 7555	AC 5AB	85558	48437	09525−0806	97.1202	0.57
ADS 7629	I 292	87416	49336	10043−2823	97.1229	0.46
CD−46 5806......	I 173	87783	49485	10062−4722	97.1175	1.71
CP−68 1034	I 13AB	88473	49764	10095−6841	97.1230	0.30[a]
CP−59 2008	HU 1597	89263	50287	10161−5954	97.1230	0.31
BD−11 2851......	RST 3688	89455	50536	10193−1232	97.1175	2.01
ADS 7846	BU 411	91881	51885	10361−2641	97.1176	0.98
ADS 7854	A 556	91962	51966	10370−0850	97.1231	2.52

TABLE 1—*Continued*

HR,ADS DM, etc. (1)	Discoverer Designation (2)	HD (3)	HIP (4)	WDS (α,δ J2000.0) (5)	Date (1900+) (6)	ΔV (7)
HR 4167	SEE 119	92139-0	51986	10373−4814	97.0903	1.61
ADS 7896	A 2768	92749	52401	10426+0335	97.1231	1.37
					97.1231	1.35
HR 4390	I 879	98718	55425	11210−5429	97.1177	1.17
ADS 8166	HU 462	99565	55875	11272−1539	97.1231	0.67[a]
CD−39 7175	I 78	100493	56391	11336−4035	97.1177	0.22[c]
CD−33 8018	HJ 4478	103192	57936	11529−3354	97.1177	0.85
					97.1177	0.84
CD−41 6849	I 80	103567	58131	11554−4154	97.0904	0.29
CP−77 772	HJ 4486	104174	58484	11596−7813	97.0905	0.67
CD−33 8130	I 215	104471	58669	12018−3439	97.1178	0.74
CD−38 7479	SEE 143	104747	58799	12036−3901	97.1232	0.37
CP−54 5306	FIN 200	110372	61982	12421−5446	97.0905	0.52
CD−47 7972	I 83	112361	63182	12567−4741	97.1178	0.30
CP−59 4740	R 213	113823	64033	13074−5952	97.1178	0.24
					97.1233	0.31
ADS 8804	STF 1728AB	114378-9	64241	13100+1732	97.1179	0.13[a]
					97.1179	0.14[c]
CD−47 8260	SLR 18	116197	65288	13229−4757	97.1234	0.38
ADS 8954	BU 932AB	118054	66247	13347−1313	97.0906	0.78[a,d]
CP−57 6143	JSP 588	117945	66285	13351−5822	97.1234	1.07
HR 5113	I 365AB	118261	66438	13372−6142	97.1179	0.35
CD−31 10706......	BU 343	120759	67696	13520−3137	97.1180	0.83
CD−35 9090	HWE 28AB	120987	67819	13535−3540	97.1234	0.48
CD−49 8475	SLR 19	123227	69012	14077−4952	97.1180	0.31
ADS 9182	STF 1819	124757	69653	14153+0308	97.1234	0.18
BD−21 3946	RST 2917	129065	71792	14411−2237	97.1235	1.23
CP−65 2914	HJ 4707	130940	72921	14542−6625	97.1180	0.57

[a] Quadrant ambiguous, but consistent with previous measures in the CHARA 3rd Catalog.
[b] Quadrant ambiguous, but inconsistent with previous measures in the CHARA 3rd Catalog.
[c] Quadrant unambiguous, but inconsistent with previous measures in the the CHARA 3rd Catalog.
[d] Astrometry for this observation was not presented in Paper I. We find $\rho = 0''.386$, $\theta = 58^\circ.9$.

photometry. This same convention is kept for all subsequent figures. We have studied the $\Delta V - \Delta H_p$ differences as a function of ΔH_p, seeing, total magnitude of the object, and the system $B-V$ color; neither the Las Campanas data nor the CTIO data exhibited significant offsets or trends.

In Figures 3 and 4, we bin the $\Delta V - \Delta H_p$ differences in seeing and ΔH_p, respectively. In the case of the seeing plots (Figs. 3*a* and 3*b*), the seeing bins are 0''.2 wide. Figure 3*a* shows the average value of $\Delta V - \Delta H_p$ as a function of seeing while Figure 3*b* shows the standard deviation of the differences in each bin. The average difference plot exhibits slightly negative trend for good seeing conditions, and then increases as the seeing deteriorates. This upturn could be due to the increasing failure of the isoplanatic assumption expected in poor seeing. The standard deviation increases dramatically between 1''.3 and 1''.5, meaning that the best

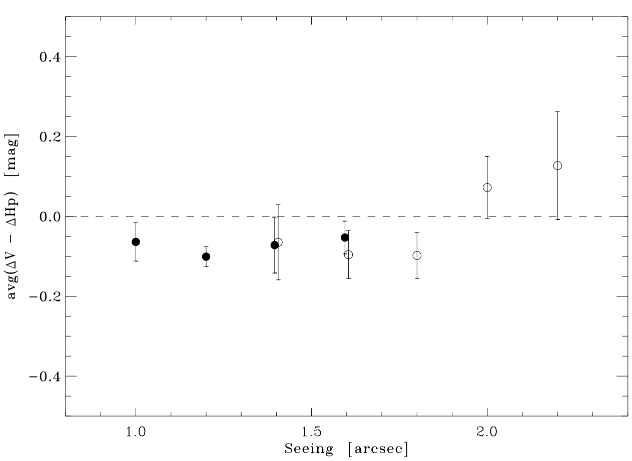

FIG. 3*a*

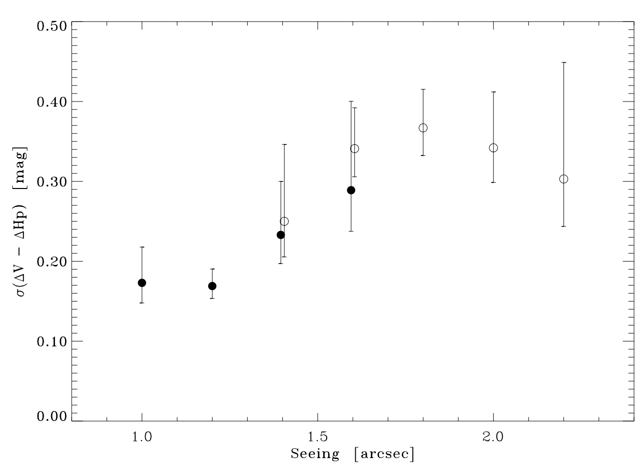

FIG. 3*b*

FIG. 3.—(*a*) Average $\Delta V - \Delta H_p$ difference plotted as a function of seeing, where observations were divided into 0''.2 wide bins. (*b*) Standard deviation of the differences using the same seeing bins. In both plots, filled circles are data points from the Las Campanas observations, and open circles are data points from CTIO.

TABLE 2

SPECKLE V-BAND DIFFERENTIAL PHOTOMETRY MEASURES, CTIO

HR,ADS DM, etc. (1)	Discoverer Designation (2)	HD (3)	HIP (4)	WDS (α,δ J2000.0) (5)	Date (1900+) (6)	ΔV (7)
HR 23	HDO 181	469	730	00090−5400	99.7676	1.05[a]
					99.7731	0.96[a]
HR 127	I 260CD	2884	2484	00316−6258	99.7676	1.28
					99.7731	1.17
					99.7786	1.43
ADS 449	MCA 1Aa	2913	2548	00324+0657	99.7867	2.31
ADS 490	HO 212AB	3196	2762	00352−0336	99.7813	1.50
					99.7950	1.38
ADS 520	BU 395	3443	2941	00373−2446	99.7650	0.76[a]
					99.7676	0.03
					99.7758	0.03[c]
BD−04 85	HDS 95	4061	3385	00430−0351	99.7813	3.37
HR 322	SLR 1AB	6595	5165	01061−4643	99.7677	0.03[a]
					99.7731	0.04[b]
HR 331	RST 3352	6767	5300	01078−4129	99.7650	1.32[c]
					99.7732	0.77[a]
					99.7732	0.80[a]
CP−55 241	RST 1205AB	6882	5348	01084−5515	99.7759	2.38
					99.7786	1.96
ADS 1123	BU 1163	8556	6564	01243−0655	99.7759	0.47[b]
CD−30 540	HJ 3447	9906	7463	01361−2954	99.7677	1.07
					99.7704	0.89
					99.7732	1.29
					99.7814	1.07
					99.7950	1.06
HR 466	KUI 7	10009	7580	01376−0924	99.7732	1.01[c]
					99.7814	1.02[c]
ADS 1339	STF 147	10453	7916	01417−1119	99.7814	1.08
ADS 1345	A 1	10508	7968	01424−0645	99.7814	1.11[b]
					99.7950	0.35[a]
ADS 1538	STF 186	11803	8998	01559+0151	99.7677	0.63[c]
					99.7705	0.63[c]
					99.7760	0.72[c]
					99.7787	0.76[c]
CD−25 979	HDS 325	15634	11644	02302−2511	99.7652	2.60
					99.7705	2.41[a]
					99.7815	2.22[a]
					99.7951	2.33[b]
ADS 2242	BU 741AB	18455	13772	02572−2458	99.7652	0.25
					99.7734	0.47[a]
HR 968	JC 8AB	20121	14913	03124−4425	99.7816	0.34
ADS 2463	SEE 23	20610	15382	03184−2231	99.7680	0.89
					99.7734	1.08
					99.7816	0.87
CP−59 298	HDS 505	25614	18731	04007−5840	99.7653	0.78[a]
HR 1357	GLE 1	27463	19917	04163−6057	99.7735	0.11[b]
ADS 3135	STT 79	27383	20215	04199+1631	99.7817	1.45[a]
ADS 3159	BU 744AB	27710	20347	04215−2544	99.7654	0.21[a]
ADS 3230	BU 311	28312	20765	04269−2405	99.7655	0.20[b]
HR 1481	KUI 18	29503	21594	04382−1418	99.7655	3.13
					99.7681	3.03
					99.7736	3.24
					99.7763	3.31
					99.7817	3.08
BD−01 702	HDS 606	29870	21894	04424−0056	99.7818	2.38
ADS 3483	BU 552AB	30869	22607	04518+1339	99.7737	2.04
					99.7763	1.98[a]
					99.7790	2.17[a]
					99.7818	1.82
ADS 3588	BU 314AB	31925	23166	04590−1623	99.7763	1.58
					99.7818	1.49
CD−35 2090	HDS 658	32846	23596	05044−3542	99.7737	2.74

TABLE 2—*Continued*

HR,ADS DM, etc. (1)	Discoverer Designation (2)	HD (3)	HIP (4)	WDS (α,δ J2000.0) (5)	Date (1900+) (6)	ΔV (7)
ADS 3711	STT 98	33054	23879	05079+0830	99.7737	1.23
					99.7763	1.03
					99.7791	1.26
					99.7818	0.99
					99.7872	1.40
ADS 3728	A 2636	33236	23957	05089+0313	99.7845	1.57
ADS 3799	STT 517AB	33883-4	24349	05135+0158	99.7845	0.57
BD+02 934	A 2641	35112	25119	05226+0236	99.7846	2.40[a]
ADS 4134	HEI 42Aa	36486	25930	05320−0018	99.7818	1.59[c]
ADS 4241	BU 1032AB	37468	26549	05387−0236	99.7846	1.06[c]
CD−48 1991	I 63AB	39177	27408	05482−4855	99.7792	1.63
BD+09 978	HEI 670	39007	27549	05500+0952	99.7764	2.59
ADS 4562	STT 124	40369	28302	05589+1248	99.7764	1.30
CD−48 2308	I 156	45572	30591	06257−4811	99.7819	1.82
CD−50 2241	R 65AB	46273	30953	06298−5014	99.7819	0.08[c]
CD−36 3031	RST 4819	47500	31637	06372−3659	99.7819	1.64
					99.7847	1.69
ADS 5487	AC 4	49662	32677	06490−1509	99.7874	1.66
HR 2937	FIN 324AB-C	61330	37096	07374−3458	99.7819	1.03
HR 3485	I 10AB	74956	42913	08447−5442	99.7820	3.38
ADS 11950	HDO 150AB	176687	93506	19026−2953	99.7864	0.31[a]
HR 7278	GLE 3	179366	94789	19172−6640	99.7754	0.65
CP−59 7534	I 121	186957	97646	19507−5912	99.7836	1.43
ADS 13104	STF 2597	188405	98038	19553−0644	99.7672	0.99[a]
					99.7755	1.68[a]
HR 7637	HO 276	189340	98416	19598−0957	99.7672	1.22[b]
ADS 14073	BU 151AB	196524	101769	20375+1436	99.7673	1.08
					99.7726	1.23
					99.7756	1.11
					99.7783	1.54[d]
					99.7837	1.19
					99.7864	1.26
ADS 14099	HU 200AB	196662	101923	20393−1457	99.7673	0.46[a]
					99.7809	0.01[a]
BD−22 5522	HDS 2957	197711	102486	20462−2145	99.7837	2.54
ADS 14360	STF 2729AB	198571	102945	20514−0538	99.7673	1.13
ADS 14499	STF 2737AB	199766	103569	20591+0418	99.7726	0.60
					99.7837	0.88
ADS 14666	STT 527	201221	104324	21080+0509	99.7810	0.92[b]
CD−41 14503......	BU 766AB	203585	105696	21244−4100	99.7811	0.13[a]
ADS 15176	BU 1212AB	206058	106942	21395−0003	99.7810	0.81
HR 8462	HDS 3152	210705	109624	22124−1412	99.7812	2.60
ADS 15902	BU 172AB	212404	110578	22241−0450	99.7812	0.20[b]
ADS 15988	STF 2912	213235	111062	22300+0426	99.7729	1.71[a]
					99.7757	1.57
					99.7811	1.49[a]
					99.7838	1.42[a]
ADS 16173	HO 296AB	214850	111974	22409+1433	99.7674	0.80[a]
CP−63 4826	I 340	216187	112924	22522−6311	99.7838	3.17
					99.7949	2.21
ADS 16365	BU 178	216718	113184	22552−0459	99.7702	1.84
					99.7948	1.56
CD−39 14936......	BU 773	218242	114132	23069−3854	99.7839	2.51
					99.7949	2.05
CD−28 18220......	HDS 3343	221083	115916	23291−2816	99.7675	1.93
BD−21 6437	B 1900	221565	116247	23333−2055	99.7729	2.64
					99.7758	2.43
CD−28 18257......	SEE 492	221839	116436	23357−2729	99.7648	1.77

[a] Quadrant ambiguous, but consistent with previous measures in the CHARA 3rd Catalog.
[b] Quadrant ambiguous, but inconsistent with previous measures in the CHARA 3rd Catalog.
[c] Quadrant unambiguous, but inconsistent with previous measures in the the CHARA 3rd Catalog.
[d] Astrometry for this observation was not presented in Paper II. We find $\rho = 0''.49$, $\theta = 339^\circ.2$.

TABLE 3

SPECKLE *R*-BAND DIFFERENTIAL PHOTOMETRY MEASURES, CTIO

HR,ADS DM, etc. (1)	Discoverer Designation (2)	HD (3)	HIP (4)	WDS (α,δ J2000.0) (5)	Date (1900+) (6)	ΔR (7)
HR 127	I 260CD	2884	2484	00316−6258	99.7839	1.40
ADS 520	BU 395	3443	2941	00373−2446	99.7650	1.09
					99.7840	0.27
					99.7950	0.00[b]
CP−61 37	HDS 107	4774	3804	00489−6022	99.7840	2.55
CP−67 62	I 48	5756	4512	00579−6634	99.7842	0.40[a]
HR 322	SLR 1AB	6595	5165	01061−4643	99.7840	0.17[b]
HR 331	RST 3352	6767	5300	01078−4129	99.7650	1.12[c]
					99.7841	1.02
CP−55 241	RST 1205AB	6882	5348	01084−5515	99.7842	2.34
CP−66 87	HDS 154	7174	5514	01106−6555	99.7950	1.89
CP−70 64	I 263	8519	6377	01220−6943	99.7950	0.80
ADS 1123	BU 1163	8556	6564	01243−0655	99.7651	0.57[b]
					99.7759	0.48[a]
					99.7840	0.49[a]
CD−48 367	RST 33	8821	6693	01259−4754	99.7841	1.36
CD−30 540	HJ 3447	9906	7463	01361−2954	99.7704	1.16
					99.7841	1.22
					99.7841	1.19
ADS 1345	A 1	10508	7968	01424−0645	99.7732	0.62
					99.7841	1.34[a]
ADS 1538	STF 186	11803	8998	01559+0151	99.7760	0.70[c]
CD−25 979	HDS 325	15634	11644	02302−2511	99.7761	2.14
					99.7869	1.94
HR 968	JC 8AB	20121	14913	03124−4425	99.7842	0.39
ADS 2463	SEE 23	20610	15382	03184−2231	99.7843	1.99
CP−59 298	HDS 505	25614	18731	04007−5840	99.7843	0.69[a]
HR 1357	GLE 1	27463	19917	04163−6057	99.7844	0.01[a]
ADS 3135	STT 79	27383	20215	04199+1631	99.7817	1.45[a]
HR 1481	KUI 18	29503	21594	04382−1418	99.7655	3.28
					99.7681	3.24
					99.7737	3.32
					99.7763	3.40
					99.7790	3.72
ADS 3483	BU 552AB	30869	22607	04518+1339	99.7737	1.74
					99.7763	1.75
					99.7790	1.86
					99.7818	1.88
CD−35 2090	HDS 658	32846	23596	05044−3542	99.7845	2.94
ADS 3711	STT 98	33054	23879	05079+0830	99.7738	1.09
					99.7763	0.90
					99.7791	1.11
					99.7819	0.88
ADS 4115	STF 728	36267	25813	05308+0557	99.7738	1.60
CD−50 2241	R 65AB	46273	30953	06298−5014	99.7873	0.31[c]
HR 2468	I 5AB	48189	31711	06380−6132	99.7874	1.48[a]
ADS 14073	BU 151AB	196524	101769	20375+1436	99.7673	0.99
					99.7726	1.10
					99.7755	1.14
					99.7783	1.44
					99.7837	0.96
					99.7864	1.20
ADS 15902	BU 172AB	212404	110578	22241−0450	99.7866	0.44[a]
ADS 15988	STF 2912	213235	111062	22300+0426	99.7757	1.37[b]
ADS 16173	HO 296AB	214850	111974	22409+1433	99.7674	0.99[a]
ADS 16365	BU 178	216718	113184	22552−0459	99.7757	2.14
					99.7867	2.09
					99.7948	1.88
CD−46 14497	HU 1335	217084	113454	22586−4531	99.7649	0.68[a]
ADS 16708	HU 295	220278	115404	23227−1502	99.7867	1.23[a]
CD−28 18257	SEE 492	221839	116436	23357−2729	99.7648	1.73

[a] Quadrant ambiguous, but consistent with previous measures in the CHARA 3rd Catalog.
[b] Quadrant ambiguous, but inconsistent with previous measures in the CHARA 3rd Catalog.
[c] Quadrant unambiguous, but inconsistent with previous measures in the the CHARA 3rd Catalog.

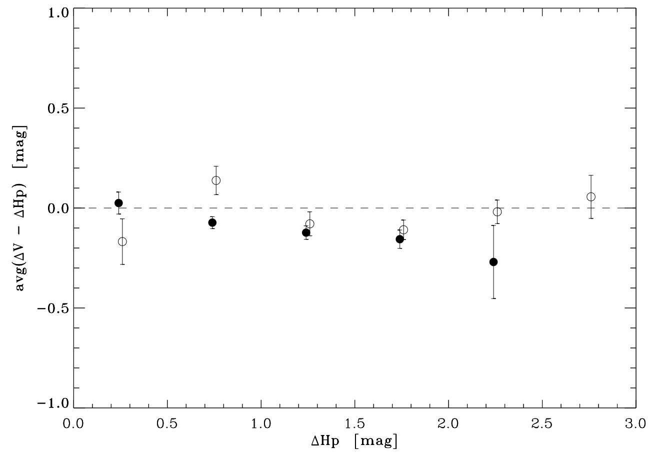

FIG. 4*a*

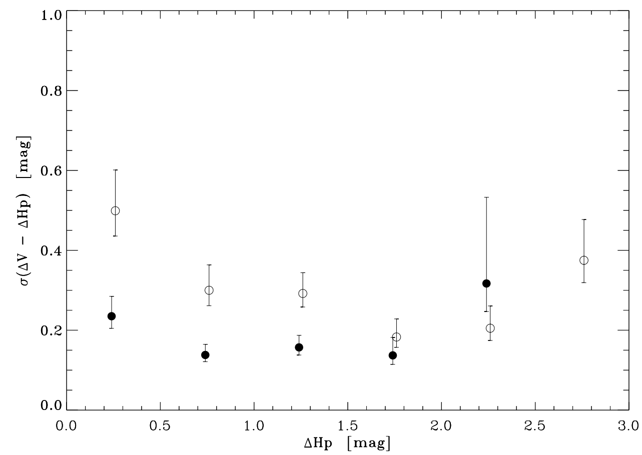

FIG. 4*b*

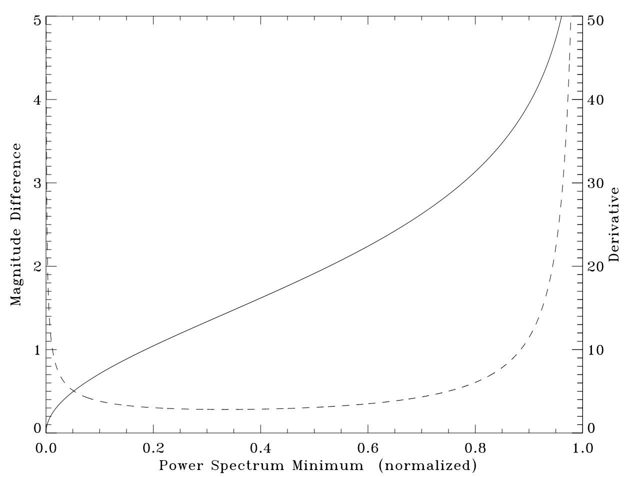

FIG. 4*c*

FIG. 4.—(*a*) Average $\Delta V - \Delta H_p$ difference plotted as a function of ΔH_p, the magnitude difference appearing in the *Hipparcos* Catalogue, where the magnitude differences were divided into 0.5 mag wide bins. (*b*) Standard deviation of the differences using the same binning. In both plots, filled circles are data points from the Las Campanas observations, and open circles are data points from CTIO. (*c*) Relationship between the power spectrum fringe minimum, $x_{\min}$, and derived magnitude difference, Δm, is shown as the solid curve (the scale of the ordinate is on the left). The dashed curve is the derivative of this function, $d(\Delta m)/dx_{\min}$, which would be relevant in error propagation (the scale for the ordinate is shown on the right).

precision in differential photometry is obtained here during the best seeing conditions. Although the two overlapping seeing bins appear consistent between the two runs, there may be other factors besides seeing (such as quality of the telescope optical system, for example) that may be contributing to this marked increase. Until more observations are taken, the plot should perhaps be viewed only as reflecting a difference between the two observing situations rather than the general behavior of photometric precision over the range of seeing shown. Figures 4*a* and 4*b* show similar plots for 0.5 mag wide bins of ΔH_p. In the average plot, no clear offsets or trends are apparent in the data set overall. In the standard deviation plot, there is an indication of lower precision (larger standard deviations) at both small and large values of ΔH_p, with a minimum at middle values ($1 \leq \Delta H_p \leq 2$). This may be due to the fact that the power spectrum fitting program is effectively estimating the depth of the interference fringes. Using equation (1), it is easy to show that, normalizing the primary irradiance, A, to 1, the minimum in the binary fringe pattern, $x_{\min}$, is related to the magnitude difference of the system by

$$\Delta m = -2.5 \log \frac{1 - \sqrt{x_{\min}}}{1 + \sqrt{x_{\min}}} . \quad (7)$$

This function has steep slopes at both large and small values of Δm, as shown in Figure 4*c*, indicating that in these regions even a small uncertainty in the power spectrum minimum will result in a large uncertainty in the magnitude difference. We are currently studying the implications of this relationship in a simulation project, and results will be forthcoming. A similar study binning the total magnitudes of the objects in 1 mag wide bins showed that the standard deviation increases at fainter magnitudes, which is consistent with signal-to-noise considerations.

Because the R bandpass is considerably redder than the H_p bandpass, a similar comparison between our R-band results and *Hipparcos* data was not completed. However, the precision of these measures is addressed in the next two subsections. Table 4 contains summary results of the V-band comparison with *Hipparcos*. We have considered two cases for each of the two observing runs, as indicated in column 2 of Table 4: first we have used every measure independently to calculate average differences and standard deviations, indicated in the column as a "1"; second, we have considered only objects observed three or more times and averaged our ΔV results before subtracting the *Hipparcos* value from it, indicated as "≥ 3" in the table. The uneven error bars in the final columns are derived from a standard chi-squared analysis. It should be noted that the *Hipparcos* measures themselves are thought to have uncertainties of approximately 0.14 mag in general (Mignard et al. 1995), so that the standard deviations presented in the plots here presumably contain errors both from *Hipparcos* and the inherent accidental errors in the speckle differential photometry. In the last column of Table 4, we have deduced our inherent measurement precision by assuming that the *Hipparcos* errors and our own add in quadrature and that the *Hipparcos* uncertainty is 0.14 mag for every case. For the Las Campanas data, we find that our measurement precision estimated in this way is $0.13^{+0.03}_{-0.02}$ mag. For the CTIO data, the result is $0.32^{+0.03}_{-0.02}$ mag. For the averaged observations, the values decrease, indicating that the behavior of our errors appears to be consistent with a stochastic

TABLE 4

SUMMARY OF V-BAND DIFFERENCES, *Hipparcos* COMPARISON

Data Set (1)	Number of Indiv. Measures (2)	Number of Objects (3)	Average Difference ($\Delta V - \Delta H_p$) (4)	rms Dev. from Ave. Diff. (5)	Subtracting 0.14 mag in Quadrature (6)
Las Campanas......	1	78	-0.08 ± 0.02	$0.19^{+0.02}_{-0.01}$	$0.13^{+0.03}_{-0.02}$
CTIO	1	109	-0.05 ± 0.03	$0.35^{+0.03}_{-0.02}$	$0.32^{+0.03}_{-0.02}$
Las Campanas......	≥ 3	3	-0.12 ± 0.09	$0.12^{+0.11}_{-0.03}$	≤ 0.20
CTIO	≥ 3	11	$+0.04 \pm 0.09$	$0.29^{+0.09}_{-0.05}$	$0.25^{+0.10}_{-0.04}$

process. Neither data set exhibits large systematic differences relative to the *Hipparcos* results, and the small negative trend is expected due to the bluer central wavelength of the H_p passband. The loss of precision in the case of the CTIO data may be at least partly related to the poorer seeing of that run relative to Las Campanas.

3.2.2. *Internal Precision*

In Tables 1, 2, and 3, there are many cases of multiple measures of various systems. We can use these as another way to estimate our internal measurement precision. In Figure 5*a*, we plot the standard deviation of ΔV for all systems observed at least three times as a function of total magnitude from the *Hipparcos* Catalogue. In Figure 5*b*, the same data are plotted as a function of the average value of the magnitude difference obtained for each system. Table 5 contains the average values of the standard deviation obtained for all three data sets given different criteria for the individual number of measures for the systems. These numbers indicate that the average internal consistency of our photometry measures is in the range 0.13–0.17 mag, consistent with the *Hipparcos* study described in the previous subsection in the case of the Las Campanas data. There are, however, two significant outliers in Figure 5. It may be that these stars are intrinsically variable, but it is also interesting to note that these systems have small magnitude differences, where according to the previous discussion one would expect a larger intrinsic scatter in the measurement of the magnitude difference. The R-band data showed a similar behavior in this regard.

TABLE 5

SUMMARY OF STANDARD DEVIATIONS, INTERNAL COMPARISON

Data Set	Req. Number of Indiv. Measures	Number of Objects	Avg. Standard Deviation
Las Campanas (V)...	≥ 3	4	0.13 ± 0.02
Las Campanas (V)...	≥ 4	3	0.14 ± 0.02
CTIO, V	≥ 3	12	0.17 ± 0.03
CTIO, V	≥ 4	8	0.14 ± 0.01
CTIO, R	≥ 3	8	0.17 ± 0.07
CTIO, R	≥ 4	4	0.14 ± 0.03

In the case of the CTIO data, the estimated internal precision is significantly lower than that of the *Hipparcos* comparison above, and indeed, the internal consistency of the Las Campanas data and the CTIO data appears quite similar. We believe that this result is at least partly due mostly to the fact that the systems with multiple observations are mainly in the range of $\Delta V = 1$ to 2.5, where according to Figure 4*b* the two data sets have much better agreement in the comparison with *Hipparcos.* Conversely, the substantially higher value of 0.3 mag for measurement precision of CTIO data may be at least partly due to the large number of small (≤ 1.0) magnitude difference systems that exist in the CTIO V-band data set. These objects contribute nearly 40% of the measures in Table 2 and have substantially higher scatter relative to the *Hipparcos* measures than the Las Campanas measures in the same ΔV bins.

3.2.3. *Comparison with Adaptive Optics Results*

Tables 1–3 also contain several objects studied by ten Brummelaar et al. (1996, 2000) using adaptive optics tech-

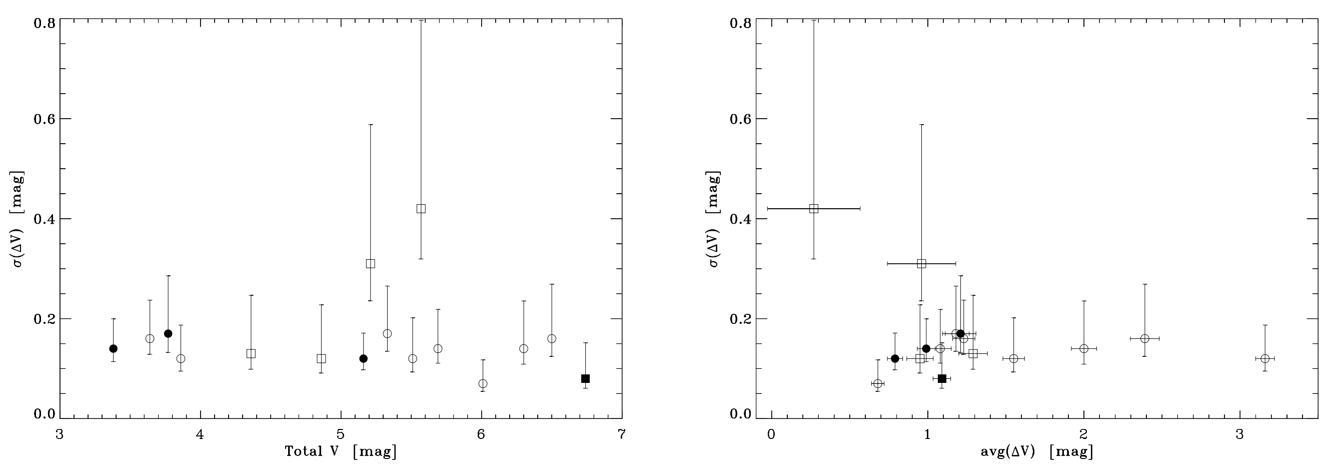

FIG. 5*a* FIG. 5*b*

FIG. 5.—(*a*) Standard deviations in V-band magnitude difference obtained in cases where the object was observed three or more times, plotted as a function of system V magnitude. (*b*) Same data plotted as a function of the average value of ΔV obtained. In both plots, squares represent systems observed only three times, while circles represent objects observed at least four times. Filled symbols indicate data from the Las Campanas observations and open symbols are objects from the CTIO data.

niques. In Figure 6, we compare our ΔV data with those results. A plot of the speckle ΔV minus the adaptive optics V-band measure, ΔV_{ao}, is shown in Figure 6*a* as a function of ΔV_{ao}, and Figure 6*b* shows the same data points plotted as a function of the system $B-V$ colors given in the *Hipparcos* Catalogue. Although the number of systems in this study is small, there appear to be no systematic offsets or trends between the two sets of results. Table 6 shows the statistical results relating to this comparison. The average difference obtained from the five systems is consistent with 0.

There are six systems from the work of ten Brummelaar et al. for which we have Bessel ΔR values in Table 3. In order to compare with their results, we have first converted the adaptive optics ΔR_{ao} values (which were in the Johnson system) to Bessel ΔR_{ao} values where possible. In order to obtain these results, we have used the transformation equation found in Fernie (1983), and assumed that the differences between the original Cousins R-band and the Bessel R are not significant. Fernie's transformation equations were used because they include uncertainty estimates for the coefficients that could be propagated along with our measurement uncertainties, but the transformations of, e.g., Bessel (1983) also give very similar results. Such transformations require the component $V-R$ colors in the Johnson system, which were available only in two cases, as shown in

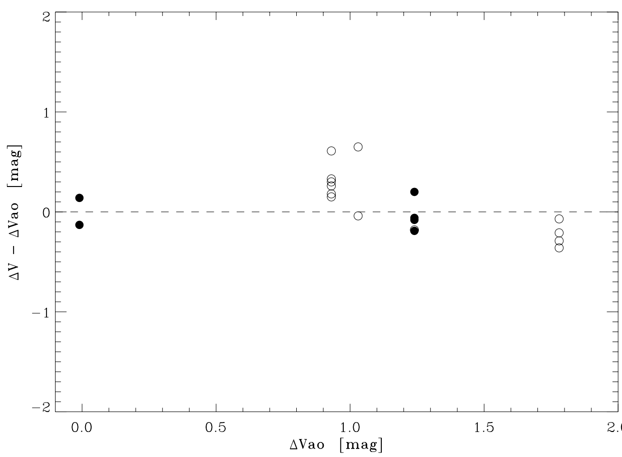

FIG. 6*a*

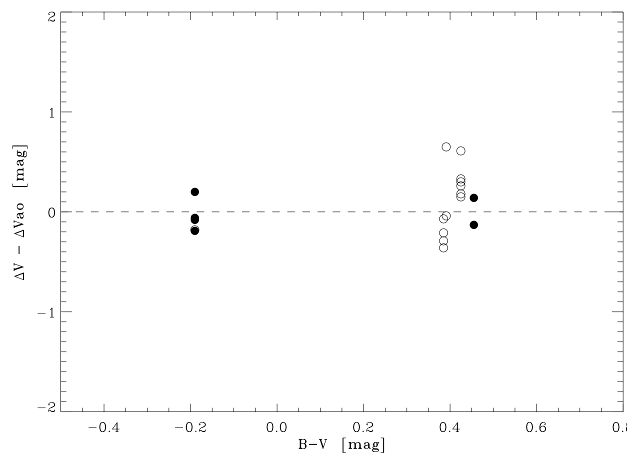

FIG. 6*b*

FIG. 6.—(*a*) V-band speckle minus adaptive optics differences plotted as a function of ΔV_{ao}, the magnitude difference result obtained in the Johnson V passband by adaptive optics, for systems with published ΔV_{ao} values. (*b*) Same differences plotted as a function of the system $B-V$ value, as it appears in the *Hipparcos* Catalogue.

TABLE 6

COMPARISON WITH ADAPTIVE OPTICS RESULTS, V-BAND MEASURES

Discoverer Designation	HIP	WDS (α,δ 2000.0)	Number of Measures	(Speckle) $\overline{\Delta V}$	ΔV_{ao}	Difference $\overline{\Delta V} - \Delta V_{ao}$
BU 1032AB.......	26549	05387−0236	5	1.18 ± 0.08	1.24 ± 0.10[a]	−0.06 ± 0.13
STF 1728AB......	64241	13100+1732	2	0.00 ± 0.19	−0.01 ± 0.06[a]	+0.01 ± 0.20
STF 2597	98038	19553−0644	2	1.34 ± 0.49	1.18 ± 0.12[a]	+0.16 ± 0.50
BU 151AB	101769	20375+1436	6	1.23 ± 0.07	0.93 ± 0.06[a]	+0.30 ± 0.09
STF 2912	111062	22300+0426	4	1.55 ± 0.07	1.78 ± 0.20[a]	−0.23 ± 0.21

[a] From ten Brummelaar et al. 2000.

TABLE 7

COMPARISON WITH ADAPTIVE OPTICS RESULTS, R-BAND MEASURES

Discoverer Designation	HIP	WDS (α,δ 2000.0)	Number of Measures	(Speckle) $\overline{\Delta R}$	Johnson ΔR_{ao}	Cousins/Bessel ΔR_{ao}	Difference $\overline{\Delta R} - \Delta R_{ao}$
STT 79..........	20215	04199+1631	1	1.45 ± 0.17	1.102 ± 0.039[b]	...	...
KUI 18	21594	04382−1418	5	3.39 ± 0.10	2.39 ± 0.23[a]	...	...
BU 552AB......	22607	04518+1339	4	1.81 ± 0.04	1.398 ± 0.031[b]	...	...
STT 98..........	23879	05079+0830	4	0.99 ± 0.07	0.719 ± 0.048[b]	...	...
BU 151AB......	101769	20375+1436	6	1.14 ± 0.08	0.98 ± 0.07[a]	0.97 ± 0.11[c]	+0.17 ± 0.14
STF 2912	111062	22300+0426	1	1.37 ± 0.17	1.54 ± 0.15[a]	1.61 ± 0.28[c]	−0.24 ± 0.33

[a] From ten Brummelaar et al. 2000.
[b] From ten Brummelaar et al. 1996.
[c] Calculated using Fernie 1983.

Table 7 along with our averaged results on the objects. Nonetheless, the average difference after comparing our Bessel ΔR values are consistent with the transformed ΔR_{ao} values from adaptive optics results.

Another way to compare the two data sets is to transform our Bessel ΔR results onto the Johnson system. This method yields lower precision than the inverse process described above due to the larger uncertainties in our photometry, but nonetheless can be completed on all six systems. In order to minimize the uncertainties, the average values of our magnitude differences from Table 7 were again used and appear in rows 3 and 4 of Table 8. In the two cases where only one measure was made (STT 79, STF 2912), uncertainties of 0.17 mag were assumed for both the speckle ΔV and ΔR. Although all the systems had total V magnitudes in the *Hipparcos* Catalogue, only one (KUI 18) had a Cousins total R magnitude listed in the General Catalogue of Photometric Data (Mermilliod, Mermilliod, & Hauck 1997). However, we were able to estimate the Bessel total R magnitudes for the other five objects using the count rates obtained during our speckle observations. These results, along with the transformations to the Johnson system for the components, again using Fernie (1983), are shown in subsequent rows of Table 8.

Plots of the speckle ΔR minus (adaptive optics) ΔR_{ao} differences as a function of magnitude difference and as a function of $B-V$ are shown in Figure 7. The result for KUI 18 appears to be discrepant relative to the adaptive optics

TABLE 8

CONVERSION TO JOHNSON R-BAND MAGNITUDES FOR SYSTEMS OBSERVED WITH ADAPTIVE OPTICS

Parameter	STT 79	KUI 18	BU 552AB	STT 98	BU 151AB	STF 2912
HIP	20215	21594	22607	23879	101769	111062
WDS	04199+1631	04382−1418	04518+1339	05079+0830	20375+1436	22300+0426
(Speckle) $\overline{\Delta V}$	1.45 ± 0.17	3.16 ± 0.06	2.00 ± 0.08	1.18 ± 0.08	1.23 ± 0.07	1.55 ± 0.17
(Speckle) $\overline{\Delta R}$	1.45 ± 0.17	3.39 ± 0.10	1.81 ± 0.04	0.99 ± 0.07	1.14 ± 0.08	1.37 ± 0.17
Total mag., V[a]	6.85 ± 0.02	3.87 ± 0.02	6.29 ± 0.02	5.32 ± 0.02	3.63 ± 0.02	5.51 ± 0.02
Total mag., Bessel R	6.99 ± 0.06[b]	3.29 ± 0.02	6.00 ± 0.06[b]	5.11 ± 0.06[b]	3.32 ± 0.06[b]	5.48 ± 0.06[b]
Primary V	7.10 ± 0.04	3.93 ± 0.02	6.45 ± 0.02	5.64 ± 0.03	3.93 ± 0.03	5.74 ± 0.04
Secondary V	8.55 ± 0.14	7.09 ± 0.06	8.45 ± 0.07	6.82 ± 0.07	5.16 ± 0.06	7.29 ± 0.14
Primary Bessel R	7.24 ± 0.07	3.34 ± 0.02	6.19 ± 0.06	5.48 ± 0.06	3.65 ± 0.06	5.75 ± 0.07
Secondary Bessel R	8.69 ± 0.15	6.73 ± 0.10	8.00 ± 0.07	6.47 ± 0.08	4.79 ± 0.08	7.12 ± 0.15
Primary Bessel $V-R$	−0.14 ± 0.08	0.59 ± 0.03	0.26 ± 0.06	0.16 ± 0.07	0.29 ± 0.07	−0.01 ± 0.08
Secondary Bessel $V-R$	−0.14 ± 0.20	0.36 ± 0.11	0.45 ± 0.10	0.35 ± 0.10	0.38 ± 0.10	0.17 ± 0.20
Primary Johnson $V-R$[c]	−0.16 ± 0.11	0.84 ± 0.04	0.39 ± 0.09	0.25 ± 0.09	0.42 ± 0.09	0.02 ± 0.11
Secondary Johnson $V-R$[c]	−0.16 ± 0.27	0.53 ± 0.16	0.65 ± 0.14	0.51 ± 0.14	0.55 ± 0.14	0.27 ± 0.27
Primary Johnson R	7.26 ± 0.12	3.09 ± 0.05	6.06 ± 0.08	5.38 ± 0.10	3.51 ± 0.10	5.72 ± 0.12
Secondary Johnson R	8.71 ± 0.31	6.56 ± 0.17	7.80 ± 0.15	6.31 ± 0.15	4.61 ± 0.15	7.02 ± 0.31
Johnson ΔR	1.45 ± 0.33	3.47 ± 0.17	1.74 ± 0.18	0.92 ± 0.18	1.11 ± 0.18	1.30 ± 0.33
Johnson $\Delta R-\Delta R_{ao}$[d]	0.35 ± 0.33	1.08 ± 0.29	0.34 ± 0.18	0.20 ± 0.19	0.13 ± 0.19	−0.24 ± 0.36

[a] Error bars of 0.02 mag are assumed in all cases.
[b] Calculated from our observations.
[c] Calculated using Fernie 1983.
[d] Using ten Brummelaar et al. 1996 and ten Brummelaar et al. 2000.

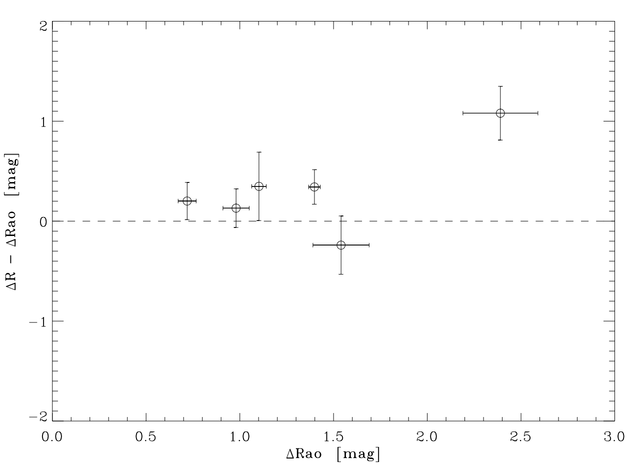

FIG. 7*a*

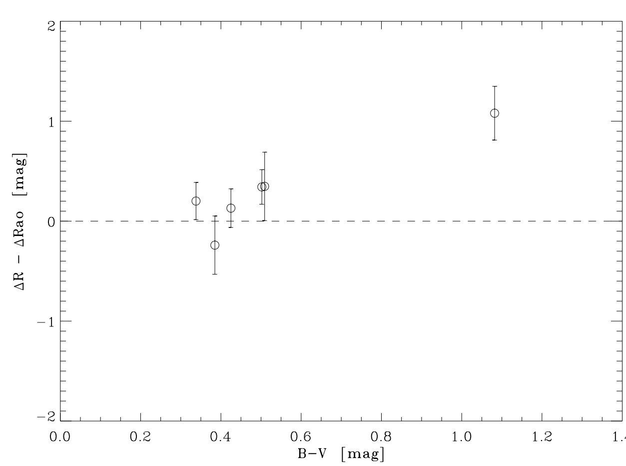

FIG. 7*b*

FIG. 7.—(*a*) Johnson R-band speckle minus adaptive optics differences plotted as a function of the adaptive optics value, ΔR_{ao}, for those systems with published ΔR_{ao} values for the six systems in Table 8. (*b*) Same differences plotted as a function of the system $B-V$ value, as it appears in the *Hipparcos* Catalogue.

result, with the speckle value presented here exhibiting a larger value of ΔR than the work of ten Brummelaar et al. (2000). The results for the other systems appear to be consistent with an average difference of 0.

3.3. *Component Magnitudes and Colors*

In four cases, the data presented here include at least four measures of the magnitude difference in both the V and R passbands. These are KUI 18, BU 552AB, STT 98, and BU 151AB, all of which are also in Table 8. The multiple measures allow us to determine average magnitude differences in these cases with smaller uncertainties, and these can then be used in combination with total V and R values to determine component magnitudes and colors with relatively good precision.

Using Table 4 in Bessel (1990), we have taken these individual component colors and estimated spectral types in the Vilnius system. Luminosity classes were not assigned except for the case of the primary in the KUI 18 system, discussed below. From Schmidt-Kaler (1982), these spectral types can then be used to obtain preliminary effective temperature estimates of the components. These are shown in Table 9, and all eight stars have been placed on the H-R diagram in Figure 8. Bolometric magnitudes were computed using the distances to the systems appearing in the *Hipparcos* Catalogue and bolometric corrections (again taken from Schmidt-Kaler) derived from the assigned spectral types. The primary in the upper right of Figure 8 is that of KUI 18; the relatively small error bars and location relative to the zero-age main sequence allowed us to assign a luminosity class of III to this object based on our photometry, consistent with the spectral classifications in both the WDS and the *Hipparcos* Catalogue. BU 151 is listed as having luminosity class IV in both catalogs; this is also consistent with the locations of the components as shown. We plan to refine results on all four systems with future observations. B-band observations would be especially helpful in reducing the formal errors in the effective temperatures and spectral types, due to the greater sensitivity of $B-V$ color on temperature compared to $V-R$.

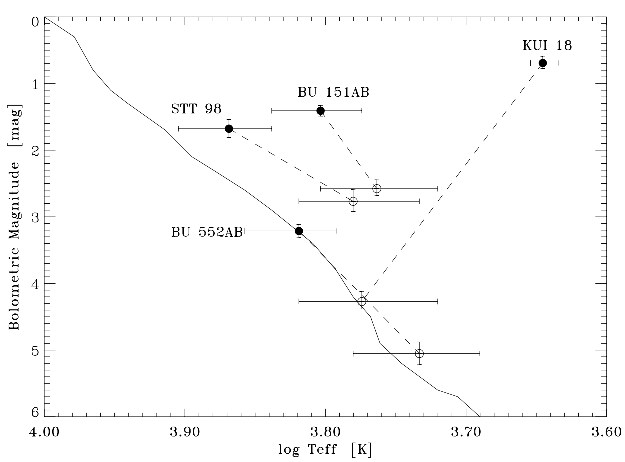

FIG. 8.—Deduced H-R diagram for the four systems with four or more observations in each filter. The filled circles represent the location of the primary, and open circles represent the location of the secondary. Dotted lines connect the primary to the secondary in each system, and the solid curve is the main sequence deduced from the bolometric magnitudes and effective temperatures in Schmidt-Kaler (1982).

4. CONCLUSIONS

Two hundred seventy-two magnitude difference estimates of binary stars have been presented, where the measures are obtained from CCD-based speckle data. A simple method for estimating the isoplanicity of an observation has been employed to insure that the magnitude differences are minimally influenced by systematic errors expected due to decorrelation of the primary and secondary speckle patterns and other effects. Further refinements of the method may be possible, but the data presented here appear to agree with values obtained by other methods.

In particular, we find that the Bessel V-band magnitude differences estimated in this way are slightly smaller than those of *Hipparcos*, as expected since the H_p passband is bluer than the V-band. Our V-band measures appear to have no significant offsets or trends relative to published adaptive optics V-band differential photometry. A study to determine the systematic effects of the R-band data was less conclusive, with our results for the system KUI 18 differing significantly from adaptive optics results. Random errors for both R and V data appear to be in the range 0.13–0.17 mag per observation, but may be substantially higher when the magnitude difference is either near 0 or very high, and/or if the seeing is poor. In the case of multiple observations, uncertainties can apparently be reduced through averaging, and this fact allowed us to estimate spectral types and effective temperatures of the components of four systems.

We are grateful to R. Millis of Lowell Observatory and R. Garrison of the University of Toronto for their support of the speckle observations; and S. Steele and F. Orrego Goya at Las Campanas and C. Enterline, O. Saa, and D.

TABLE 9

SPECTRAL TYPES AND EFFECTIVE TEMPERATURE ESTIMATES FOR SYSTEMS OBSERVED AT LEAST FOUR TIMES IN V AND IN R

Parameter	KUI 18	BU 552AB	STT 98	BU 151AB
Assigned spectrum, primary	K2 III	F4	A9	F6
Range	K1.5 III–K2.5 III	F0–F8	A6–F2	F2–G1
Assigned spectrum, secondary	G1	G9	G0	G4
Range	F4–K0	G0–K2	F4–G9	F6–K0
Primary $T_{\rm eff}$	4420^{+90}_{-110}	6590^{+610}_{-390}	7390^{+635}_{-500}	6360^{+530}_{-415}
Secondary $T_{\rm eff}$	5945^{+645}_{-695}	5410^{+620}_{-510}	6030^{+560}_{-620}	5800^{+560}_{-550}

Maturana of CTIO for their help during the observing runs. William van Altena and Reed Meyer of Yale University also provided helpful comments. We thank the referee for a thoughtful reading of the manuscript and for suggested improvements. This work was funded by two small grants from NASA administered by the American Astronomical Society and JPL Subcontract 1201846 from the Preparatory Science Program for the Space Interferometry Mission.

REFERENCES

Bagnuolo, W. G., Jr. 1988, Opt. Lett., 13, 907
Bagnuolo, W. G., Jr., & Sowell, J. R. 1988, AJ, 96, 1056
Barnaby, D., Spillar, E., Christou, J. C., & Drummond, J. D. 2000, AJ, 119, 378
Bessel, M. S. 1983, PASP, 95, 480
———. 1990, PASP, 102, 1181
Dainty, J. C. 1984, in Laser Speckle and Related Phenomena, ed. J. C. Dainty (New York: Springer), 255
Dombrowski, E. G. 1990, Ph.D. thesis, Georgia State Univ.
ESA. 1997, The *Hipparcos* and Tycho Catalogue (ESA SP-1200) (Noordwijk: ESA)
Fernie, J. D. 1983, PASP, 95, 782
Hartkopf, W. I., Mason, B. D., McAlister, H. A., Turner, N. H., Barry, D. J., Franz, O. G., & Prieto, C. M. 1996, AJ, 111, 936
Hartkopf, W. I., McAlister, H. A., & Mason, B. D. 1997, Third Catalog of Interferometric Measurements of Binary Stars, CHARA Contribution No. 4 (Atlanta: Georgia State Univ.)
Hoffleit, D., & Jaschek, C. 1982, The Bright Star Catalogue (4th ed.; New Haven: Yale Univ. Obs.)
Horch, E., Franz, O. G., & Ninkov, Z. 2000, AJ, 120, 2638 (Paper II)
Horch, E. P., Ninkov, Z., & Slawson, R. W. 1997, AJ, 114, 2117 (Paper I)
Mermilliod, J.-C., Mermilliod, M., & Hauck, B. 1997, A&AS, 124, 349
Mignard, F., et al. 1995, A&A, 304, 94
Roberts, L. C., Jr. 1998, Ph.D. thesis, Georgia State Univ
Schmidt-Kaler, T. 1982, in Landolt-Börnstein New Series, Group 6, Vol. 2b, Stars and Star Clusters, ed. K. Schaifers & H.-H. Voigt (Berlin: Springer), 1
ten Brummelaar, T. A., Hartkopf, W. I., McAlister, H. A., Mason, B. D., Roberts, L. C., Jr., Turner, N. H. 1998, Proc. SPIE, 3353, 391
ten Brummelaar, T. A., Mason, B. D., Bagnuolo, W. G., Jr., Hartkopf, W. I., McAlister, H. A., & Turner, N. H. 1996, AJ, 112, 1180
ten Brummelaar, T. A., Mason, B. D., McAlister, H. A., Roberts, L. C., Jr., Turner, N. H., Hartkopf, W. I., & Bagnuolo, W. G., Jr. 2000, AJ, 119, 2403
Worley, C. E., & Douglass, G. G. 1997, A&AS, 125, 523